Original Article

Yishen Xiezhuo formula ameliorates the development of cisplatin-induced acute kidney injury by attenuating renal tubular epithelial cell senescence

Qiaoying Zhang, Jieying Qi, Qin Luo, Mengni Wu, Lili Zhang, Linsen Qin, Xiaoli Nie

Department of Nephrology, Integrated Hospital of Traditional Chinese Medicine, Southern Medical University, Guangzhou, China

Contributions: (I) Conception and design: Q Zhang, X Nie; (II) Administrative support: J Qi, Q Luo; (III) Provision of study materials or patients: M Wu; (IV) Collection and assembly of data: L Zhang; (V) Data analysis and interpretation: Q Zhang, L Qin; (VI) Manuscript writing: All authors; (VII) Final approval of manuscript: All authors.

Correspondence to: Xiaoli Nie. Department of Nephrology, Integrated Hospital of Traditional Chinese Medicine, Southern Medical University, Guangzhou, China. Email: nxl117@163.com.

Background: Although cisplatin (DDP) is an important clinical anti-tumor drug, its use is limited by its nephrotoxicity. How to avoid the renal injury incurred by platinum drugs and improve the clinical efficiency of platinum drugs use has become an urgent clinical problem. Previous studies have verified that Chinese medicine has definite effects on acute kidney injury (AKI). Yishen Xiezhuo formula (YSXZ) is a traditional Chinese medicine (TCM) compound which is an effective clinical drug for AKI, but its mechanism remains unclear.

Methods: In our research, an AKI model was induced by DDP in human renal tubular epithelial cell (HKC) lines in the *in vitro* study. The mechanism of the YSXZ on cell senescence was analyzed by Cell Counting Kit-8 (CCK-8), senescence-associated β-galactosidase (SA-β-Gal) staining, western blot, flow cytometry, and enzyme-linked immunosorbent assay (ELISA). Network pharmacology was used to analyze the role of YSXZ against AKI.

Results: Compared with the control group, the cells in the DDP intervention group were significantly senescent. Compared with DDP group, YSXZ decreased the number of SA-β-Gal-positive senescence cells, down regulated the expression of senescence-related proteins, reduced the release of senescence-related secreted phenotypic factors, and reversed the phenomenon of cell cycle S-phase arrest. Network pharmacology and experimental studies showed that the mitogen-activated protein kinase (*MAPK*) signaling pathway played a central role.

Conclusions: Our present results suggested that YSXZ ameliorated the development of DDP-induced AKI by attenuating renal tubular epithelial cell (RTEC) senescence via alleviating the activation of *MAPK* pathway.

Keywords: Yishen Xiezhuo formula (YSXZ); cisplatin (DDP); acute kidney injury (AKI); cell senescence; network pharmacology

Submitted Sep 30, 2022. Accepted for publication Dec 20, 2022.

doi: 10.21037/atm-22-5415

View this article at: https://dx.doi.org/10.21037/atm-22-5415

Introduction

Cisplatin (DDP) is an important anti-tumor drug, which has achieved good effects in the treatment of lung cancer, testicular cancer, gastric cancer, and other malignant tumors (1-3). However, with the increase of clinical use, the probability of toxic side effects of platinum drugs has also greatly increased, among which renal toxicity is the most typical (4-7). According to statistics, despite the preventive

use of hydration therapy, more than 30% of patients continue to experience different degrees of renal injury (8). Moreover, a study (9) has found that the incidence of kidney injury in patients with chronic kidney disease (CKD) and tumors is significantly higher than that in patients with tumors only when using platinum-based drugs. How to circumvent renal injury incurred and improve the efficiency of platinum drugs in clinical use has become an urgent problem.

Renal tubular epithelial cells (RTECs) are the most important executors of renal function and the mainly damaged cells in AKI. When the injury is relatively mild, the remaining RTECs show a transient adaptive regeneration phenotype and mature RTECs are produced through proliferation and differentiation, thus enabling the recovery of renal function. On the other hand, when the damage is severe or persistent, RTECs cannot complete normal proliferation and differentiation under maladjustment repair, and continue to secrete inflammatory factors and fibrogenic factors, leading to irreversible damage to the renal structure. The mechanisms include mitochondrial dysfunction, cell cycle arrest, cellular senescence, as well as epithelial-mesenchymal transition (EMT). Recent study shows that the use of platinum drugs makes the RTECs continue to repair poorly and the expression of necrosis and apoptosis-related proteins increase, directly inducing that the acute reversible kidney injury develops into chronic, irreversible kidney disease (10). Therefore, the damage and repair of RTECs is the core link affecting the outcome of AKI.

In recent years, study has shown that the risk of nephrotoxicity induced by platinum drugs in elderly patients is 1.43 times higher than that in non-elderly patients (11). Therefore, it seems that the mechanism of platinum drugs amplifying renal injury sensitivity is closely related to cell senescence. Cell senescence is widespread in nature and is mainly manifested in the degradation and loss of a series of functions at the molecular, cellular, tissue, and organ levels; permanent and stable proliferation arrest are the prominent features (12). Cell senescence can be divided into replicative senescence (RS) and stress-induced senescence. RS refers to the circumstance when cells are cultured *in vitro*, the number of mitosis increases, and after reaching the Hayflick limit, cells stop dividing. RS of cells is often accompanied by telomere shortening, which is a natural biological process (BP) (13). Stress-induced premature senescence (SIPS) refers to the premature aging of cells under a series of internal and external stimuli, such as the accumulation of reactive oxygen species (ROS), DNA damage, and the activation of protooncogenes, often without telomere shortening. In recent years, it has been found that cell senescence is closely related to the occurrence of various diseases (14), among which, after acute kidney injury (AKI), RTECs can undergo stress-induced senescence, resulting in poor kidney repair, which is one of the important mechanisms of AKI chronicity. Al-Dabet *et al.* (15) found that under the stimulation of high glucose, ROS production in RTECs increased, which induced DNA damage reaction (DDR), making p21 and γ-H2AX continuously overexpress, causing SIPS. What's more, Yang *et al.* (16) characterized the cell cycle profile of tubular epithelial cells in several vivo AKI models, including ischemia-reperfusion injury (IRI), severe IRI, unilateral IRI, acute aristolochic acid toxic nephropathy (AAN) and unilateral ureteral obstruction (UUO). The result showed that the development of AKI models correlated with the arrest of proximal tubule epithelial cells in G2/M and the upregulation of profibrotic gene expression and collagen production. Observably, delaying RTEC senescence is of great significance for impeding and interfering with the chronicity of AKI.

Presently, the measures to prevent cisplatin (DDP) induced nephrotoxicity mainly include hydration, diuresis, magnesium supplementation, organic cation transporter 2 (OCT2) inhibitors (cimetidine or metformin), and high-dose glutathione (17-19). However, even with the above measures, the incidence of DDP induced nephrotoxicity is still high. According to various promising laboratory findings, many natural products (flavonoids, saponins, alkaloids, etc.) and traditional Chinese medicine (TCM) compounds showing potent medicinal properties can protect the kidney against injury (20). Astragaloside IV (AS IV) is an active compound of the Traditional Chinese Herb Astragalus membranaceus, and has been shown to be protective against DDP-induced liver and kidney

Highlight box

Key findings

- Network pharmacology revealed that *MAPK* pathway was an important pathway for treatment of cisplatin-induced AKI with YSXZ by attenuating RTEC senescence.

What is known and what is new?

- YSXZ effectively ameliorates cisplatin-induced AKI.
- The mechanism of YSXZ in ameliorating cisplatin-induced AKI is closely related to attenuating cell senescence via *MAPK* pathway.

What is the implication, and what should change now?

- YSXZ is of great value in the treatment of cisplatin-induced AKI.

injury by inhibiting the expression of NOD-like receptor family pyrin domain containing 3 (NLRP3) and blocking the release of pro-inflammatory cytokines (21). Shenkang injection (SKI), a Chinese patent medicine injection, is effective to DDP-induced AKI and elucidates by inhibiting inflammation and oxidative stress (22). This opens up a new way to study the preventive measures against DDP-induced by nephrotoxicity.

Yishen Xiezhuo formula (YSXZ) is composed of 4 herbs: Astmgali Radix, Sargassum, Alismatis Rhizoma, and Radix Paeoniae Rubra. Astmgali Radix is used as the principal drug in the kidney and the ministerial drugs are Alismatis Rhizoma and Radix Paeoniae Rubra. Sargassum is used as the assistant. The whole prescription has the function of tonifying Qi, unblocking the collaterals, removing turbid water, and discharging water. The formula has achieved certain efficacy in the treatment of AKI caused by DDP, but its mechanism has not been elucidated.

Therefore, this study was designed to establish an AKI *in vitro* model of RTECs stimulated by DDP, and to provide a theoretical basis for the treatment of DDP-induced AKI with YSXZ. We present the following article in accordance with the MDAR and ARRIVE reporting checklists (available at https://atm.amegroups.com/article/view/10.21037/atm-22-5415/rc).

Methods

Molecular biological validation

Preparation of YSXZ aqueous extract

YSXZ was provided by the Pharmacy Department of Integrated Hospital of Traditional Chinese Medicine, Southern Medical University (Guangzhou, China) and consisted of the following herbs: 1,000 g Astmgali Radix, 500 g Sargassum, 500 g Alismatis Rhizoma, and 500 g Radix Paeoniae Rubra. Decoction tablets of all herbs were decocted twice after soaking in cool water for 30 minutes, and separation of the solid and liquid parts was performed in a hot state. The concentration was carried out under reduced pressure and at a temperature below 65 ℃, followed by freeze-drying. Finally, 526.22 g water extract-lyophilized powder was obtained and the rate of wastage was 30%.

Preparation of YSXZ drug-containing serum

Sprague-Dawley rats (male), weighing (250±50 g), were granted from SPF (Beijing) Biotechnology Company [Beijing, China; quality certificate number: SCXK(Jing)2019-0010]. The rats received gavage once a day for 7 days with the prepared dosage of YSXZ (rat YSXZ serum, n=6) or distilled water (rat con serum, n=6). Six rats were housed per cage and all rats received food and water ad libitum under controlled environmental conditions (room temperature 20±3 ℃, room humidity 40–60%, background noise 40±10 dB, 12:12 h light-dark cycles) for 3 days to adapt to the environment. The therapeutic dose for rats was 6.25 times higher than that for patients based on body weight. Blood was collected from the abdominal aorta 2 hours after intragastric administration on day 7. Prior to blood collection, rats were administered chloral hydrate intraperitoneally at a dose of 0.3 mL/100 g. After anesthesia, to locate the abdominal aorta, the abdominal cavity of the rats was surgically opened. Blood was then collected as much as possible from the abdominal aorta using a disposable blood collection needle and a negative pressure blood collection tube, and the serum were extracted using a centrifuge at 3,500 rpm for 15 minutes. Both rat YSXZ serum and rat con serum were mixed, sterilized in a water bath at 56 ℃ for 30 minutes. and stored at –80 ℃. Animal experiments were performed under a project license (No. L2022-065) granted by Laboratory Animal Welfare and Ethics Committee of Integrated Hospital of Traditional Chinese Medicine, Southern Medical University, and was carried out in compliance with the relevant regulations of the Experimental Animal Ethics and Welfare Committee of Southern Medical University. A protocol was prepared before the study without registration.

Cell culture

Human RTEC lines (HKC; RRID:CVCL_Y910) were a gift from the team of Professor Zhou Lili from the National Clinical Research Center for Nephrology (Guangzhou, China). Cells were cultured in Dulbecco's Modified Eagle Medium/F-12 (DMEM/F12; A4192301; Gibco, Grand Island, NY, USA) supplemented with 10% fetal bovine serum (FBS; BI, 04-001-1A, Kibbutz, Israel) and 1% penicillin-streptomycin (P1400; Solarbio, Beijing, China). Cells were cultured at 37 ℃ in a 5% CO_2 atmosphere. All experiments were performed after 2 passages.

Cell Counting Kit-8 (CCK-8) assay

The HKC cells 100 μL/well (5×10^4 cells/mL) were plated in 96-well plates and incubated in a moistened incubators at 37 ℃ and 5% CO_2 overnight. The cells were incubated with DDP (0, 5, 10, 20, and 40 μM) for 6 hours, and then incubated in complete medium for 18 hours. Meanwhile,

they were treated with YSXZ drug-containing serum (2.5%, 5%, 10%, 20%, and 40%) for 24 hours. Then, 10 μL of CCK-8 (GK10001; GLPBIO, Montclair, NJ, USA) was added to each well, and the cells were incubated on the condition of 37 ℃, 5% CO_2 for 4 hours. Eventually, the absorbance was measured at 450 nm by a microplate reader (RRID:SCR_019749; BioTek, Waltham, MA, USA) and the rate of cell proliferation inhibition was calculated.

Measurement of the activity of senescence-associated β-galactosidase (SA-β-Gal)

Cell senescence was identified based on the instruction manual of the SA-β-Gal staining kit (C0602; Beyotime Biotechnology, Beijing, China). In short, the cells were inoculated into 24-well plates at 7×10^4 cells per well and treated with DDP alone or in combination with YSXZ. The cells were fixed at ambient temperature for 15 minutes after washing with cold phosphate-buffered saline (PBS) 3 times. Then, 500 μL SA-β-Gal solution was added to each well and cells were incubated at 37 ℃ overnight after washing again. Finally, cells were photographed by electron microscope. ImageJ software (RRID:SCR_003070; National Institutes of Health, Bethesda, MD, USA) was used to count SA-β-Gal-positive cells.

Analysis of cell cycle in HKC

A Cell Cycle Analysis Kit (C1052; Beyotime Biotechnology) was used to analyze the cell cycle in HKC. Cells were digested and suspended by trypsin without ethylenediamine tetraacetic acid (EDTA) at a concentration of 10×10^5 cells/mL. Subsequently, the suspended cells were plated out overnight in 35 mm culture plates at a volume of 1 mL per plate and then treated with the specified dosages of DDP and YSXZ. Then, cells were collected and fixed overnight at 4 ℃ in 70% ice-cold ethanol. After washing with PBS, cells were incubated with propidium iodide (PI) stain solution at room temperature for 30 minutes and then subjected to flow cytometry [FACS CantoTM, Beckton Dickinson (BD) Biosciences, San Jose, CA, USA]. To determine the cell cycle progression, data obtained were evaluated by the FlowJo software (V10, RRID:SCR_008520; BD Biosciences)

Western blotting

Treated-HKC were lysed in radioimmunoprecipitation assay (RIPA) lysis buffer on ice for 30 minutes after washing 3 times with ice-cold PBS. The bicinchoninic acid (BCA) assay kit (P0012S; Beyotime Biotechnology) was used to determine the total protein concentration. A total of 20 μg of protein was then separated at 120 V on an 12% sodium dodecyl sulfate-polyacrylamide gel electrophoresis (SDS-PAGE) separator. Proteins were subsequently transferred to a 0.22 μm polyvinylidene fluoride (PVDF) membrane (03010040001; Millipore, Billerica, MA, USA). The PVDF membranes were blocked at room temperature for 2 hours by tris-buffered saline with Tween 20 (TBST) comprising 5% bovine serum albumin (BSA) and incubated with primary antibodies, including histone H2AX (*γ-H2AX*) [RRID:AB_2800054; Cell Signaling Technology (CST) Cat# 85410], cyclin-dependent kinase inhibitor 2A (*p16*) (RRID:AB_2833600; Affinity Biosciences Cat# BF0580), cyclin-dependent kinase inhibitor 1 (*p21*) (RRID:AB_2827699; Affinity Biosciences Cat# AF6290), cellular tumor antigen p53 (*p53*) (RRID:AB_2881401; Proteintech Cat# 60283-2-Ig), c-Jun N-terminal kinase (*JNK*) (RRID:AB_2835178; Affinity Biosciences Cat# AF6319), extracellular regulated protein kinases 1/2 (*ERK1/2*) (RRID:AB_2139967; Abcam Cat# ab54230), phospho-extracellular regulated protein kinases (*p-ERK1/2*) (RRID:AB_2139990; Santa Cruz Biotechnology Cat# sc-16982), p38MAPK (*p38*) (RRID:AB_307202; Abcam Cat# ab9352), phospho-p38MAPK (*p-p38*) (RRID:AB_2141746; Santa Cruz Biotechnology Cat# sc-166182), phosphatidylinositide 3-kinases (*Pi3K*) (RRID:AB_562192; Abcam Cat# 1593-1), phospho-phosphatidylinositide 3-kinases (*p-Pi3K*) (RRID:AB_10789447; Antibodies-Online Cat# ABIN461415), serine/threonine-protein kinase AKT (*Akt*) (RRID:AB_722674; Abcam Cat# ab18785), phospho-serine/threonine-protein kinase AKT (*p-Akt*) (RRID:AB_10805010; Antibodies-Online Cat# ABIN461540), and glyceraldehyde-3-phosphate dehydrogenase (*GAPDH*) (RRID:AB_2107436; Proteintech Cat# 60004-1-Ig) overnight at the temperature of 4 ℃. According to the manufacturer's instructions, each antibody was diluted. We washed the PVDF membrane with TBST 3 times. The membrane was then incubated with secondary antibodies at room temperature for 2 hours. Eventually, we used the Tanon 5200s (Tanon, Shanghai, China) to measure the intensity of the immunoreactive bands. Image J and SPSS software (IBM Corp., Armonk, NY, USA) were used to analyze the data.

Enzyme-linked immunosorbent assay (ELISA)

As an indicator of senescence-associated secretory phenotype (SASP), the amount of interleukin-6 (*IL-6*) and interleukin-1β (*IL-1β*) in cell culture supernatants was measured using commercial ELISA kits (EHC007.48,

EHC002b.48; NeoBioscience Biotechnology, Shenzhen, China). Supernatants were collected after centrifugation (2,500 rpm) at 4 ℃ for 10 minutes and added to an antibody 96-well plate which was coated with antibody. Subsequently, the antibody labeled with horseradish peroxidase (HRP) was added into the plate. Afterwards, the plate was chromogenized with 3,3',5,5'-tetramethylbenzidene (TMB), and the optical density (OD) value was detected with a microplate reader (RRID:SCR_019749; BioTek Thermo Fisher Scientific, Waltham, MA, USA) at a wavelength of 450 nm. Finally, the contents of *IL-6* and *IL-1β* were calculated by the standard curve.

Network pharmacology analysis of YSXZ

Database and analysis software

Databases including Traditional Chinse Medicine Systems Pharmacology (TCMSP; https://old.tcmsp-e.com/tcmsp.php), Genecards (https://www.genecards.org/), UniProt (https://www.uniprot.org/), the Search Tool for the Retrieval of Interacting Genes/proteins (STRING; https://cn.string-db.org/), Bioinformatics (https://www.bioinformatics.com.cn/), Metascape (https://metascape.org/gp/index.html), Online Mendelian Inheritance in Man (OMIM; https://omim.org/), Therapeutic Target Database (TTD; http://db.idrblab.net/ttd/), and Disgenet (https://www.disgenet.org/) were used to collect data. The data were analyzed by Cytoscape software (v3.8.2., RRID:SCR_003032; https://cytoscape.org/).

Chemical components of YSXZ

The TCMSP online database (23) was utilized in search of chemical constituents of YSXZ. The compounds were screened and analyzed according to absorption, distribution, metabolism, and excretion (ADME)-related indicators. Among which, components with an oral bioavailability (OB) ≥30% and drug-like properties (DL) ≥0.18 were considered potentially useful and were thereafter be screened based on the "five rules" (24) proposed by Lipinski.

Construction of YSXZ-compounds-targets network

The relationships between herbal medicines, potentially bioactive compounds, and targets associated with the compounds were vividly displayed by Cytoscape software (v3.8.2.; RRID:SCR_003032).

Collection and Identification of AKI-related targets

The AKI-related targets were collected using the following terms: "Acute Kidney Injury" AND "Acute Kidney Insufficiency" AND "Acute Kidney Failure" AND "Acute Renal Injury" AND "Acute Renal Insufficiency" AND "Acute Renal Failure" AND "Acute Kidney Tubular Necrosis" AND "acute on chronic kidney disease". Targets were retrieved from GeneCards (25), OMIM (26), TTD (27), and Disgenet (28).

Construction and modular analysis of protein-protein interaction (PPI) networks

By the means of Venn diagram established by the Bioinformatics database, the overlapping targets of the YSXZ and AKI were captured and considered candidate targets. A PPI network of the original candidate targets was created by STRING (29) in order to determine the relationship between the imported protein-coding genes. "Homo sapiens" was set as the biological species, the minimum threshold for interactions was set to "highest confidence" (>0.9), and other settings were set as default. Cytoscape 3.8.2 was used to draw the common targets PPI network. According to the degrees in the diagram, the node size and color are adjusted. Cluster analysis was performed by the Molecular Complex Detection (MCODE) tool. the analysis parameter set to default and the MCODE score set to 2. After analysis, the module was adjusted and displayed in the chart.

Functional annotation and enrichment analyses of YSXZ

Gene Ontology (GO) analysis, including molecular functions (MFs), BPs, and cellular components (CCs), is a widely accepted method for defining and describing genes. The Kyoto Encyclopedia of Genes and Genomes (KEGG) is a vast collection of databases on genomes, drugs, enzymes, biological pathways, and more. Metascape (30) was used to perform GO and KEGG enrichment analysis for both clusters, with adjusted P values <0.01 as the cutoff.

Statistical analysis

All the above experiments were performed in 3 independent replications. All data were expressed in the form of the mean ± standard deviation (SD) of 3 independent experiments. Comparisons between multiple groups were performed by one-way analysis of variance (ANOVA) with least significant difference (LSD) test when the variance was homogeneous and Dunnetts T3 test when the variance was not homogeneous. Enumeration data were expressed as

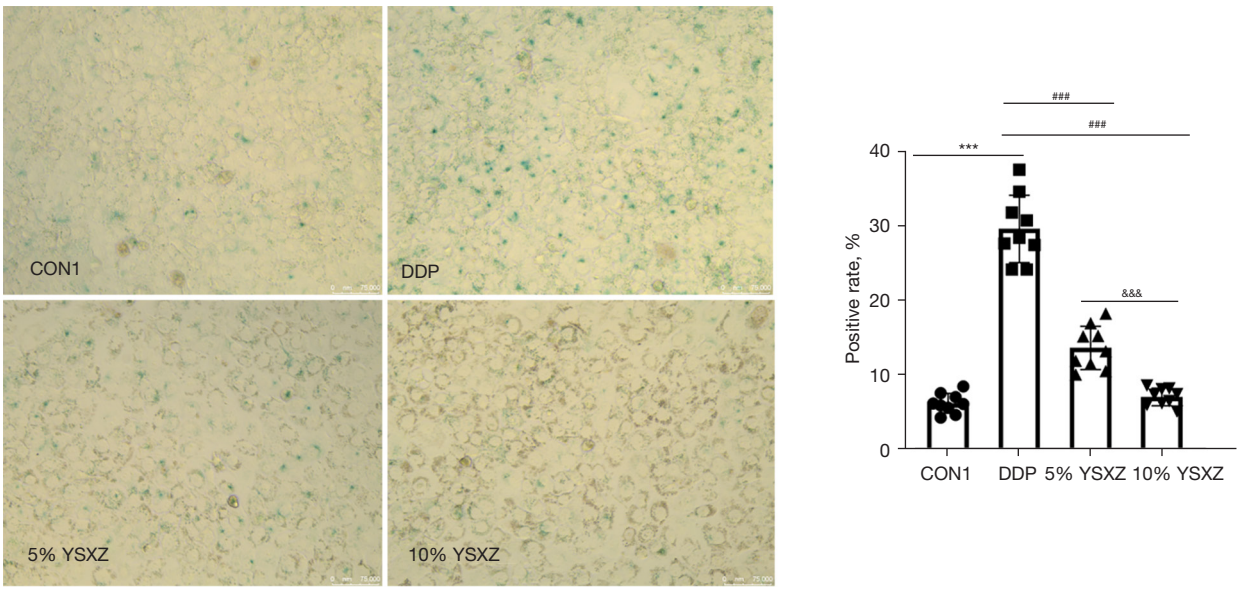

Figure 1 The effect of YSXZ on the SA-β-Gal activity of HKC treated with DDP. SA-β-Gal staining was conducted and cells with positive nuclear staining (blue-green) represent senescence (under 200× magnification). The data are presented as the mean ± SEM. (n=9). ***P<0.001 compared to the CON1 group; ###P<0.001 compared to the DDP group; &&&P<0.001 compared to the 5% YSXZ group. CON1 represents FBS control. DDP, cisplatin; YSXZ, Yishen Xiezhuo formula; SA-β-Gal, senescence-associated β-galactosidase; HKC, human renal tubular epithelial cells; SEM, standard error of the mean; FBS, fetal bovine serum.

number (proportion) and were analyzed by Chi-square test or Fisher exact test. All data were statistically analyzed using SPSS 23.0 (RRID:SCR_002865; IBM Corp., Armonk, NY, USA), and P<0.05 was considered statistically significant. In addition, GraphPad Prism v9.4.1 (RRID:SCR_002798; GraphPad Software, San Diego, CA, USA) was responsible for visualization.

Results

YSXZ attenuated RTEC senescence

Effects of different concentrations of DDP and YSXZ on the activity of RTECs

After stimulating HKC cells with different concentrations of DDP (0, 5, 10, 20, and 40 μM) for 6 hours, the drug was withdrawn, and all wells were replaced with complete medium containing 10% FBS. Afterwards, in order to find the optimal drug concentration (Figure S1A), and determine whether YSXZ has a toxic effect on HKC cells, we used different concentrations of YSXZ-containing serum (1.25%, 2.5%, 5%, 10%, 20%, and 40%) to intervene cells. The cell proliferation activity was detected by CCK-8 method at 24 hours (Figure S1B).

Based on the results of the above experiments, we performed subsequent experiments by 25 μM DDP and 5% or 10% YSXZ.

YSXZ decreased the number of SA-β-Gal-positive senescence cells

SA-β-Gal is considered a specific marker of cell senescence, and cells with positive nuclear staining (blue-green) represent senescence. The results showed that the number of cells in the DDP group was apparently less than that in the control group. The cell volume and nuclear volume were significantly increased, and the cells showed a large and flat senescence-like morphology. Cellular senescence was determined by a SA-β-Gal staining assay. DDP markedly induced cell senescence, and the DDP group had a higher proportion of SA-β-Gal-positive cells than the control group (P<0.001). YSXZ (5%, 10%) significantly improved the ageing of HKC induced by DDP in a concentration-dependent manner (P<0.001) (*Figure 1*).

YSXZ down-regulated the expression level of senescence proteins in HKC

p16 and *γ-H2AX* are recognized as eukaryotic cell senescence markers. The up-regulating expression of *p53*

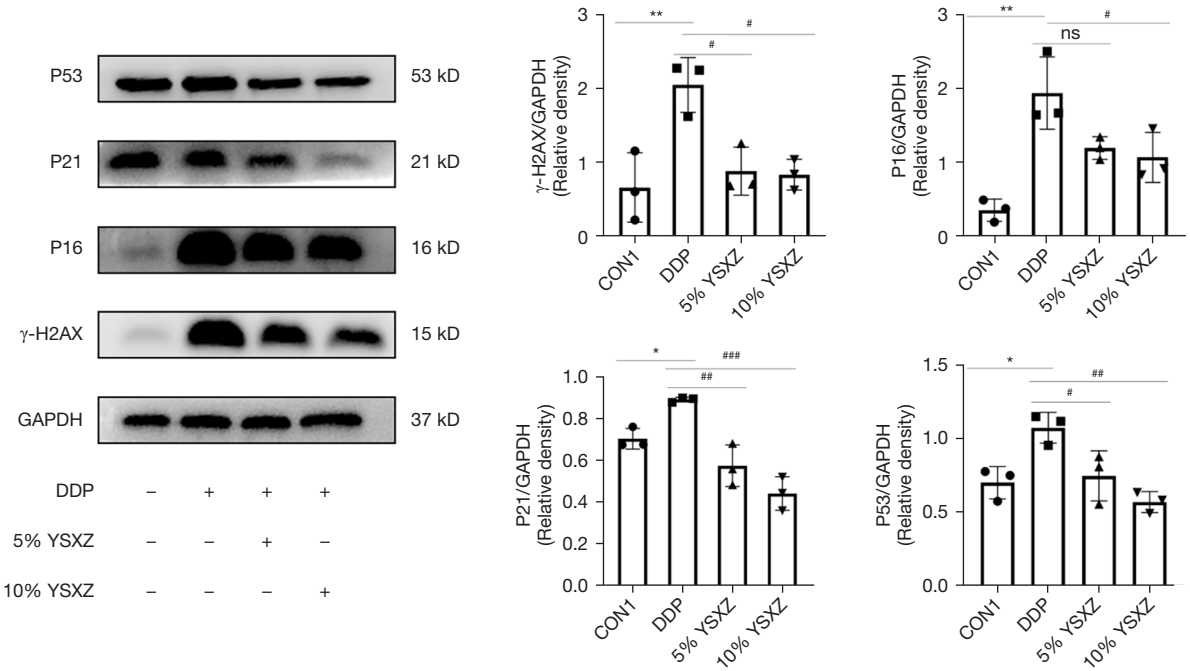

Figure 2 Expression of senescence-related proteins of each group. **P<0.01, *P<0.05 compared to the CON1 group; ###P<0.001, ##P<0.01, #P<0.05 compared to the DDP group; ns, no significant. CON1 represents FBS control. DDP, cisplatin; YSXZ, Yishen Xiezhuo formula; FBS, fetal bovine serum.

and *p21* is closely related to cell cycle arrest. The results showed significantly increased expression of *γ-H2AX*, *p16*, and *p53* compared to controls (P<0.05). The expression of related proteins was markedly decreased after YSXZ intervention (P<0.05), and the effect of 10% YSXZ was more obvious (*Figure 2*). Combining the results of SA-β-Gal staining and aging-related protein expression, 10% was determined to be the optimal concentration of YSXZ.

YSXZ reversed the cell cycle arrest of HKC induced by DDP

Afterward, to explore the effect of YSXZ on the cell cycle of HKC after DDP intervention, cell cycle distribution was assessed by flow cytometry. The results showed that the cells in the DDP group were arrested in the DNA replication phase (S phase) compared to the control group. However, compared with DDP group, the proportion of S-phase cells in the YSXZ treatment group decreased significantly, and the proportion of G2 phase cells increased, indicating that the YSXZ can reverse the S-phase arrest of HKC cells induced by DDP (*Figure 3*).

YSXZ reduced the SASPs abnormal secretion of HKC

SASPs, characteristic secretions of senescent cells, have been reported to disrupt the microenvironment and promote disease progression. Therefore, we measured the concentration of 2 representative SASPs, including *IL-1β* and *IL-6*. The results showed that the intervention of YSXZ circumvented the increase of these SASPs (*Figure 4*).

Network pharmacology analysis of the possible mechanism of YSXZ

Active ingredients and targets of YSXZ

Based on the TCMSP databases, 62 active ingredients of YSXZ were screened, including 20 compounds from Astmgali Radix, 10 from Alismatis Rhizoma, 29 from Radix Paeoniae Rubra, and 4 from Sargassum (Table S1). Based on these active ingredients in YSXZ, 154 active ingredients-related targets were acquired via TCMSP. We used the Cytoscape 3.8.2 software to construct the network visualization diagram of the active ingredient target of YSXZ (*Figure 5*).

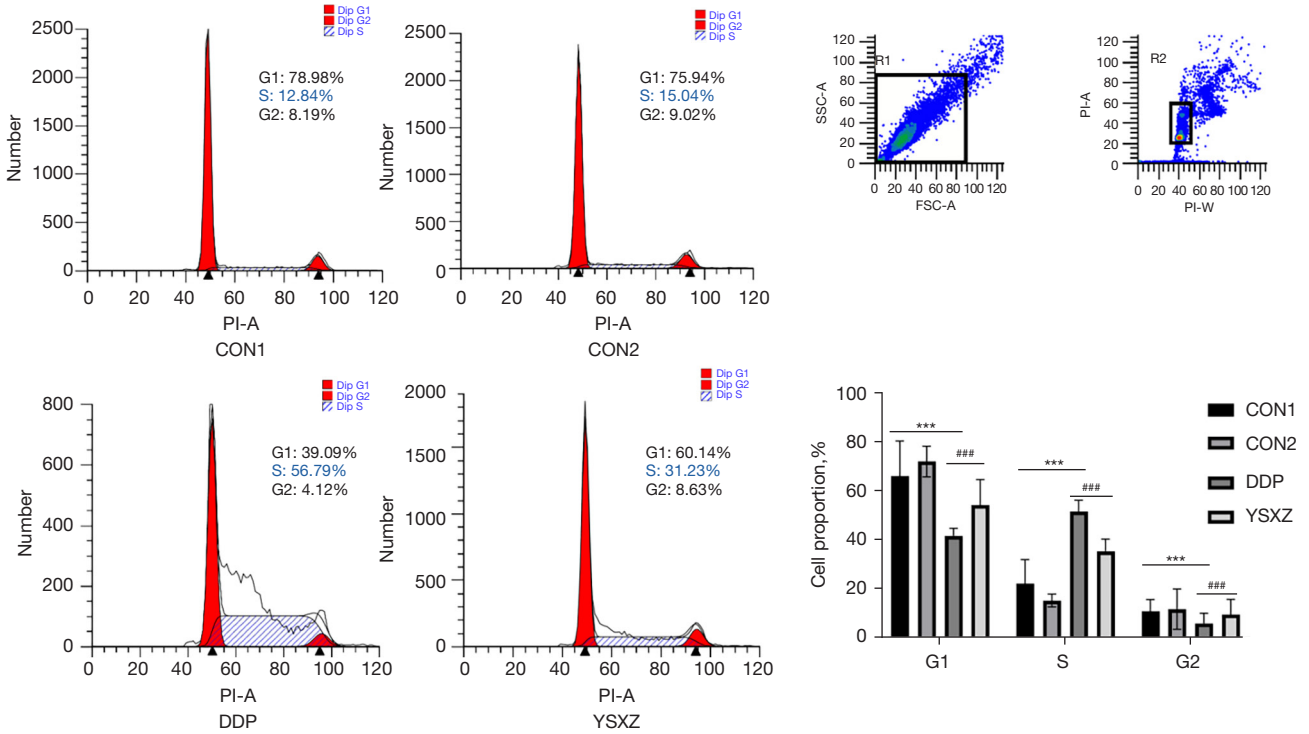

Figure 3 The cell cycle distribution of each group. ***P<0.001 compared to the CON1 group; ###P<0.001 compared to the DDP group. CON1 represents FBS control; CON2 represents YSXZ drug-containing serum control. PI, propidium iodide; SSC-A, side-scatter area; FSC-A, forward-scatter area; DDP, cisplatin; YSXZ, Yishen Xiezhuo formula; FBS, fetal bovine serum.

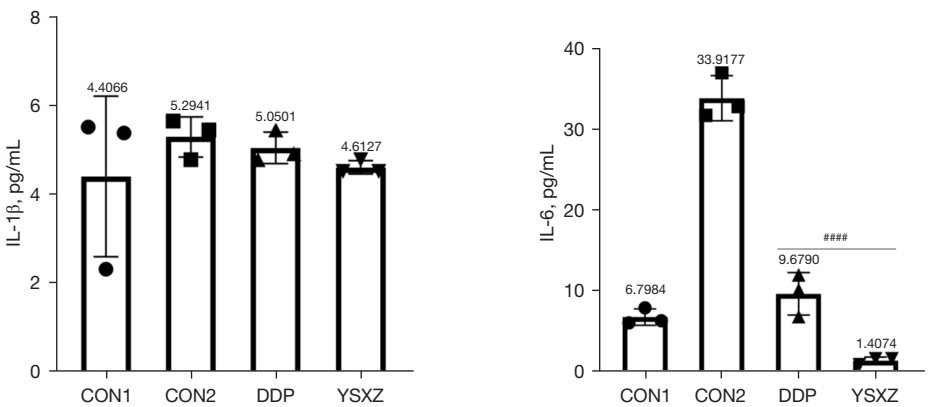

Figure 4 The concentrations of IL-1β and IL-6 in the supernatant of cell culture medium of each group. ####P<0.0001 compared to the DDP group. CON1 represents the FBS control; CON2 represents YSXZ drug-containing serum control. IL-1β, interleukin-1β; DDP, cisplatin; YSXZ, Yishen Xiezhuo formula; IL-6, interleukin-6; FBS, fetal bovine serum.

Target collection of AKI and active ingredients of YSXZ

After merging the 5 disease database targets and deleting the duplicate values, 12,647 AKI-related targets were finally obtained. The active ingredient target of YSXZ and the target of AKI were intersected, and the Venn diagram was drawn using the online software Venny 2.1.0.90 (*Figure 6*). Finally, the common targets of YSXZ and AKI were

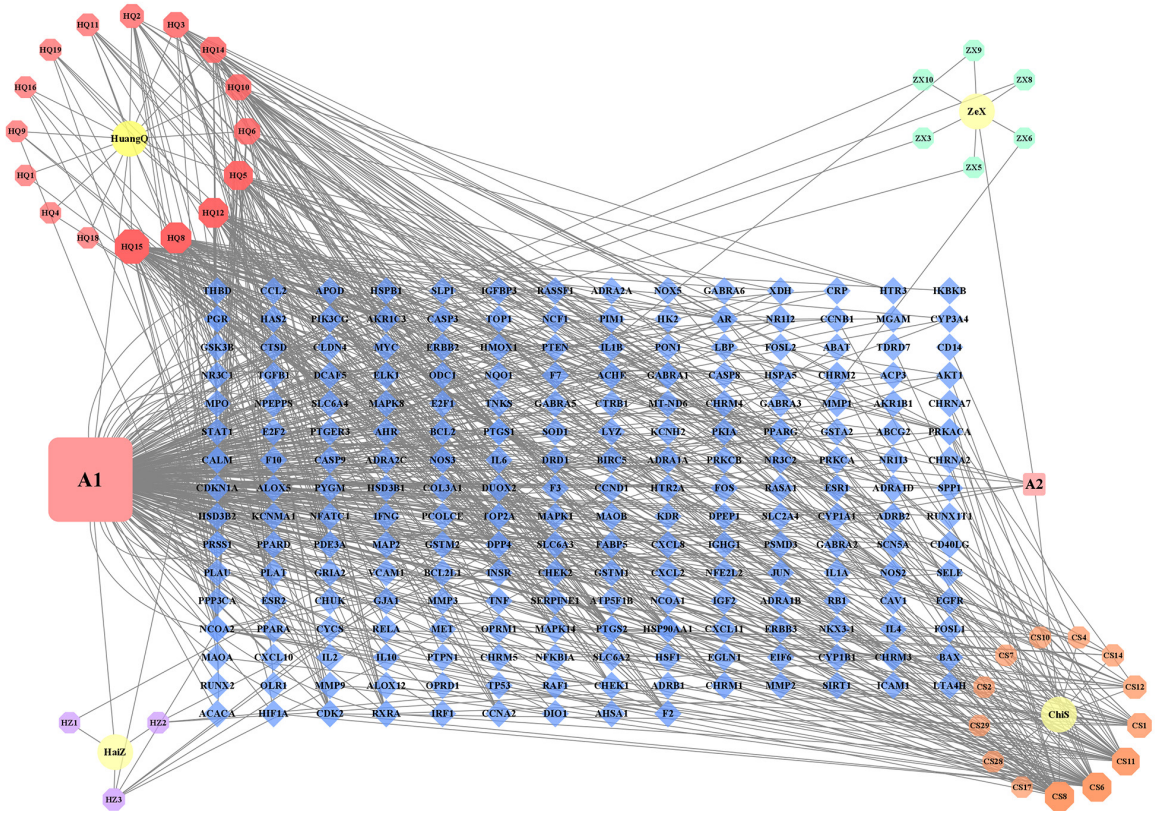

Figure 5 A network diagram was constructed using Cytoscape. The yellow circles represent four herbs of YSXZ. The red, green, purple, and orange circles represent the active ingredients of the four herbs in YSXZ. The pink squares represent the common ingredient between 4 herbs. The full list of corresponding active ingredients is shown in Table S1. The blue diamonds represent YSXZ-related genes, and the edges represent interactions between ingredients and target genes. YSXZ, Yishen Xiezhuo formula.

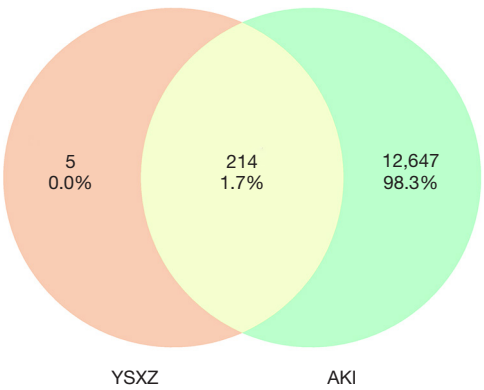

Figure 6 Venn diagram of proteins associated with YSXZ and AKI. The overlapping genes were considered as potential hub genes for YSXZ in the treatment of AKI. YSXZ, Yishen Xiezhuo formula; AKI, acute kidney injury.

obtained (Table S2).

Construction of YSXZ target-AKI network

A PPI network is composed of individual proteins interacting with each other and is the basis of various intracellular mechanisms. Construction of PPI networks allows a systematic analysis of the interaction relationships among numerous proteins *in vivo* to understand the functional principles, the reaction mechanisms of biological signals, and energy metabolism in diseases and other special physiological conditions. Based on the identified YSXZ- and AKI-related target genes, we constructed a Venn diagram with YSXZ and AKI-related proteins. The overlapped genes were designated as differentially expressed genes (DEGs), which are potential hub genes for the effect

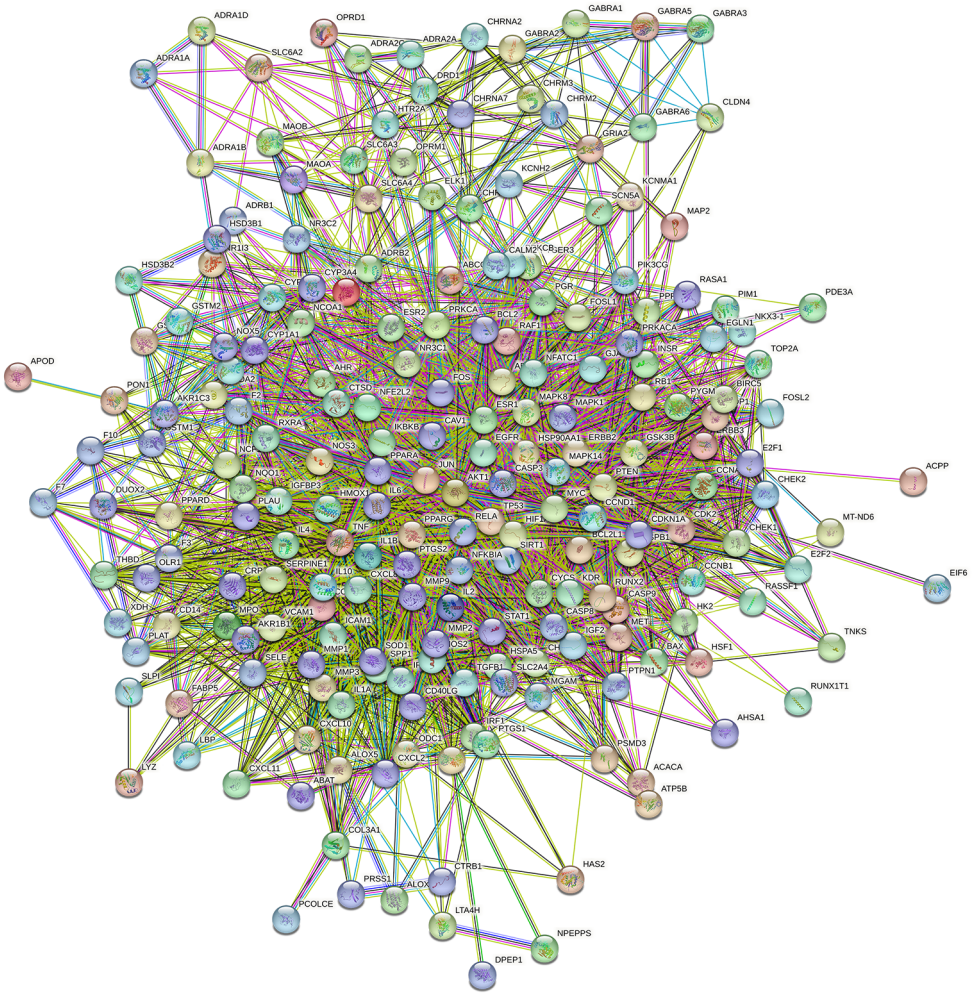

Figure 7 The PPI analysis of 214 overlapping targets of YSXZ and AKI. The nodes get larger with an increasing degree. Edges: PPI between shared targets and their interactive partners. PPI, protein-protein interaction; YSXZ, Yishen Xiezhuo formula; AKI, acute kidney injury.

of YSXZ on AKI. A total of 214 DEGs hypothesized to be associated with the effect of YSXZ on AKI were filtered into the PPI network complex. In addition, a PPI network of 214 DEGs was created (*Figure* 7). There are 177 nodes and 757 edges in the network. After analyzing the network, the average value of the node degree is 8.964. Among them, the top 5 nodes in terms of degree are: JUN, HSP90AA1, MAPK1, TP53, RELA (*Table 1* for node details). In cluster analysis, there are top 10 modules with an MCODE score of 2 (*Table 2* for module details).

GO function and KEGG pathway enrichment analysis

GO items were obtained from the Metascape database. The top 20 BP, CC, and MF catalogs were then selected and visualized (*Figure 8A*). In the histograms, the normal axis represents the degree of enrichment. According to our BP results, the function of the active components of YSXZ in AKI were mainly concentrated in response to inorganic substance, response to hormone, response to xenobiotic stimulus, cellular response to lipid, response to decreased oxygen levels, positive regulation of CC movement, response to extracellular stimulus, inflammatory response, positive regulation of cell death, and circulatory system process. The MF items mainly included DNA-binding transcription factor binding, protein domain specific binding, nuclear receptor activity, kinase binding, protein homodimerization activity, postsynaptic neurotransmitter receptor activity, adrenergic receptor activity, protein

Table 1 Targets in protein-protein interaction network of YSXZ and AKI (top 5)

Name	Degree	Average shortest path length	Betweenness centrality	Closeness centrality
JUN	43	2.060606	0.096449	0.485294
HSP90AA1	39	2.187879	0.09287	0.457064
MAPK1	39	2.042424	0.12548	0.489614
TP53	38	2.212121	0.092755	0.452055
RELA	37	2.133333	0.057195	0.46875

YSXZ, Yishen Xiezhuo formula; AKI, acute kidney injury.

Table 2 Modules of the PPI network of common targets of YSXZ and AKI

Module	Targets	MCODE score	Nodes	Edges
1	TNF, CXCL2, CCL2, CXCL8, CXCL10, IL1A, RELA, IL1B, IL4, IL6, IL10	10	11	50
2	TGFB1, MMP2, LBP, MMP9, MMP1, MMP3	5.6	6	14
3	PIM1, RXRA, ESR1, SIRT1, PPARA, NOS2, MYC, MAPK14, HIF1A, BIRC5, NR3C1, TP53, CDK2, E2F1	5.231	14	34
4	GABRA5, GABRA3, GABRA6, GABRA2, GABRA1	5	5	10
5	HSD3B2, CYP3A4, HSD3B1, AKR1C3	4	4	6
6	AR, MAPK8, HSPB1, BAX, EGFR, CYCS, MAPK1, ELK1, CASP9, CD40LG, AKT1, CASP3	3.818	12	21
7	RUNX2, RB1, CAV1, INSR, JUN, ADRA1B, IGFBP3, CDKN1A, NFE2L2, F2, CHUK, CHRM1, FOSL1, PRKCA, IGF2, ADRB2, FOS, ESR2, PRKCB, GSTA2, PTPN1, IKBKB	3.81	22	40
8	SELE, ICAM1, VCAM1	3	3	3
9	F10, F7, F3	3	3	3
10	ALOX5, PTGS1, ALOX12	3	3	3

PPI, protein-protein interaction; YSXZ, Yishen Xiezhuo formula; AKI, acute kidney injury; MCODE, Molecular Complex Detection.

kinase activity, oxidoreductase activity, and cytokine receptor binding. The CC items focused on membrane raft, postsynaptic membrane, receptor complex, transcription regulator complex, dendrite, dendrite membrane, side of membrane, ion channel complex, vesicle lumen, and protein kinase complex. The abundant GO functions may also help to explain, to some extent, the potential use of YSXZ in the treatment of AKI and other diseases. KEGG pathway enrichment analysis revealed that YSXZ was primarily involved in multiple important signaling pathways (*Figure 8B*). The 10 most enriched metabolic pathways were plotted in a bubble diagram, with the horizontal axis representing gene enrichment score, the size of the bubble representing gene numbers, and the color intensity representing P value. The most important enriched metabolic pathways were pathways in cancer, lipid and atherosclerosis, chemical carcinogenesis-receptor activation, the mitogen-activated protein kinase (*MAPK*) signaling pathway, chemical carcinogenesis-ROS, the *Pi3K-Akt* signaling pathway, pathways of neurodegeneration-multiple diseases, platinum drug resistance, the *HIF-1* signaling pathway, and the calcium signaling pathway.

Verification of the *MAPK* and *Pi3K/Akt* pathways

Next, the *MAPK* pathway and *Pi3K/Akt* pathways with high correlation obtained from KEGG analysis were verified. The results showed that *JNK* expression in the DDP group was significantly increased compared with the control group, and the phosphorylation ratio of *ERK1/2* and *p38* was significantly up-regulated. YSXZ could down regulate *JNK* expression and reduce the phosphorylation ratio of *ERK1/2* and *p38* after intervention. For the *Pi3K* pathway, after

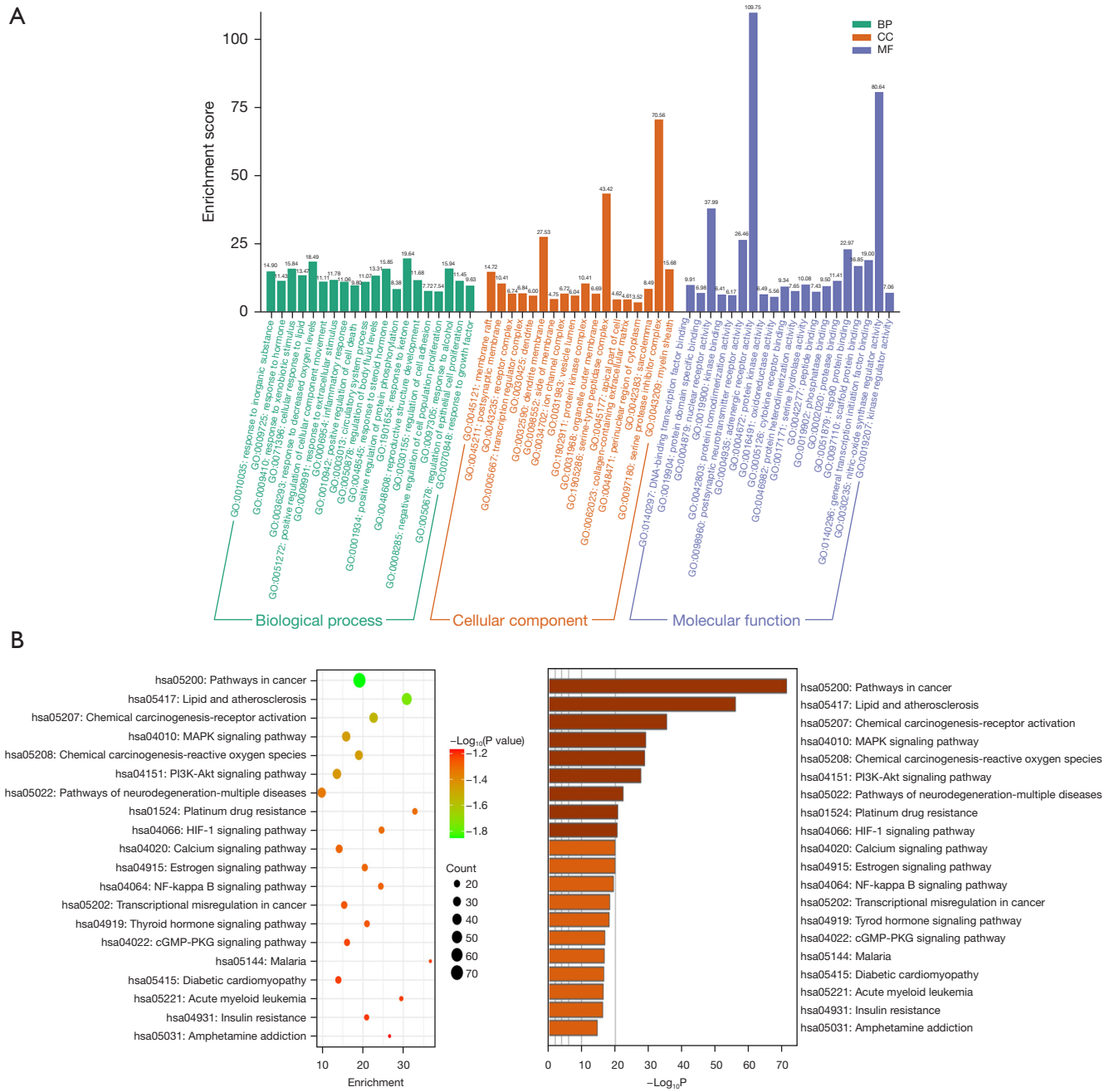

Figure 8 GO function and KEGG pathway enrichment analysis of YSXZ in AKI treatment. (A) GO function analysis including BP, CC, and MF. (B) Bubble diagram of the enrichment of KEGG pathways. BP, biological process; CC, cellular component; MF, molecular function; GO, Gene Ontology; KEGG, Kyoto Encyclopedia of Genes and Genomes; YSXZ, Yishen Xiezhuo formula; AKI, acute kidney injury.

DDP stimulation, the total expression and phosphorylation ratio of *Pi3K* were not significantly different from those of the control group; the phosphorylation ratio of *Akt* was up-regulated, but there was no improvement after the intervention of YSXZ (*Figure 9A*,*9B*). From this, we can infer that the YSXZ may play a role through *MAPK*

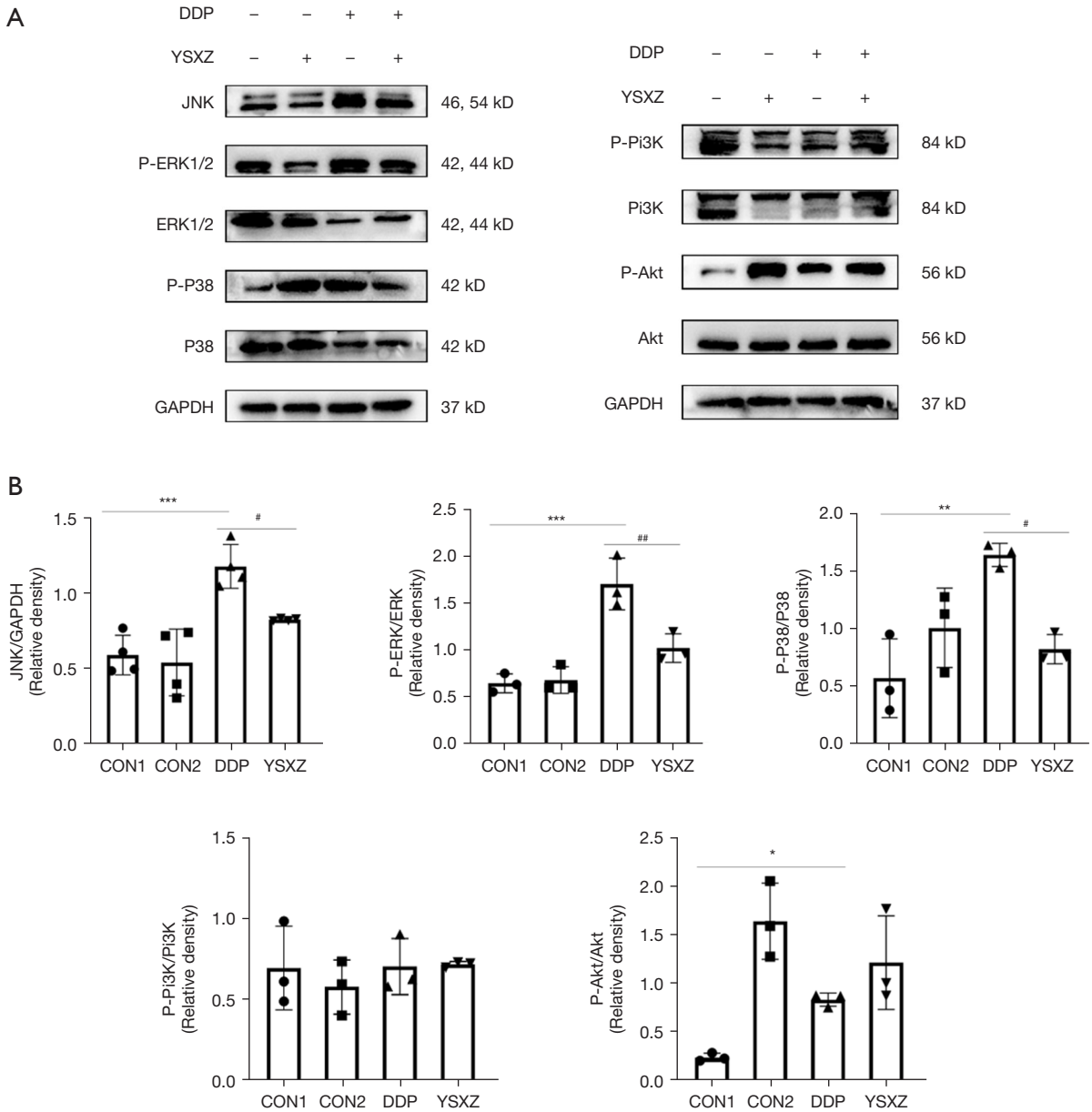

Figure 9 YSXZ was able to interfere with *MAPK* signaling in DDP-induced HKC. (A) The effect of YSXZ on *MAPK* and *Pi3K/Akt* signaling pathways was detected by Western blotting. (B) Protein expression of related proteins in HKC was analyzed by Western blotting. The results were quantified by densitometry. Data are presented as mean ± SD (n=3 per group) of the representative data from three independent experiments. ***P<0.001, **P<0.01, *P<0.05 compared to the CON1 group; ##P<0.01, #P<0.05 compared to the DDP group. CON1 represents FBS control; CON2 represents YSXZ drug-containing serum control. DDP, cisplatin; YSXZ, Yishen Xiezhuo formula; *MAPK*, mitogen-activated protein kinase; HKC, human renal tubular epithelial cells; SD, standard deviation; FBS, fetal bovine serum.

pathway in delaying DDP-induced renal injury.

Discussion

It is very easy for DDP to accumulate in the kidneys. The concentration of DDP in RTECs at the proximal end of the kidney is about 5 times higher than that of serum. Therefore, nephrotoxicity has become the most common side effect of platinum drugs (31). Many clinical and experimental articles on platinum-mediated nephrotoxicity

have shown that unbound platinum will be filtered through the glomeruli and transported to the RTECs, resulting in renal tubular injury and dysfunction, reducing glomerular filtration rate, segmental degeneration, necrosis, and shedding and accumulation of proximal and distal renal tubules (32). For DDP-induced renal injury, there is still a lack of more effective treatment methods, except for renal replacement therapy and hydration therapy, which have a certain effect. It is of great clinical significance to exploit the wealth of TCM and explore a TCM-based scheme for the treatment of DDP-induced kidney injury that is "simple, effective, cheap, and convenient".

In recent years, it has been found that the mechanism of platinum drugs-mediated kidney injury is closely related to cell senescence. Senescent cells are mainly characterized by the following features: cells lose their regular shape, become large and flat, and their nuclei are sunken (33); senescence-associated heterochromatin foci (SAHF) formation (34); up-regulation of aging related proteins; SA-β-Gal activity increases (35); SASPs such as *IL-1β* and increased secretion of *IL-6* (36); cell cycle arrest, and so on (33,37). Current study asserts that cell senescence caused by platinum drugs may be closely related to the destruction of mitochondrial structure, the production of ROS, and DNA damage. Li *et al.* (38) stimulated NRK-52E cells with 20 μm DDP for 6 hours, removed the drug, and continued to culture in complete medium for 24, 48, and 72 hours. After that, the SA-β-Gal positive rate increased to 15% at 48 hours and 22% at 72 hours. Cell cycle analysis by flow cytometry showed that 20 μm DDP resulted in a significant increase in the percentage of cells arrested in S phase and a significant upregulation of cyclin *p53* and *p21* proteins. It is suggested that DDP can cause cell cycle arrest and premature aging by mediating DNA damage response. However, the specific mechanism behind it remains to be explored.

YSXZ is modified from Shenbing decoction III, which is based on the 40 years clinical experience of Professor Ren Luo, a famous old Chinese medicine practitioner in China. Shenbing decoction III has been proved to effectively reduce the excretion of urine protein in CKD patients, improve their renal function, and effectively delay the process of renal failure (39). YSXZ selected the four most important herbs in Shenbing decoction III and adjusted its prescription dosage in compliance with the *Pharmacopoeia of the People's Republic of China*. That is 30 g Astmgali Radix, 15 g Sargassum, 15 g Alismatis Rhizoma, and 15 g Radix Paeoniae Rubra. Modern pharmacological research shows that AS IV may protect against DDP-induced AKI by decreasing the inflammatory response, reducing oxidative stress, and improving energy metabolism (40). Alginate Oligosaccharide can alleviate DDP-induced kidney oxidative stress via Lactobacillus Genus-FAHFAs-Nrf2 Axis in mice (41). From this point of view, YSXZ has the potential to treat AKI caused by DDP and many other kidney diseases.

For a long time, drug development strategies have assumed that a single target mechanism of action is the best choice for target specific therapy, which is selective in treating specific diseases without adverse effects (42,43). However, in clinical practice, herbal medicine exists in the form of formula. That is, multiple herbal medicines are combined into one prescription, which is called "Fang" in TCM. Its dosage size and dosage form are quite complex in application scenarios. According to the characteristics of the disease with different symptoms, various herbs or herbal combinations can be added or reduced. Therefore, the treatment of TCM has the characteristics of multi-components and multi-targets (44-46).

Network pharmacology can realize the integration of medicine, biology, computer science, and other disciplines. It is characterized by the "disease-phenotype-gene-drug" interaction network and focuses on the comprehensive and systematic study of the mechanism of drug intervention on the disease network, which coincides with the holistic view of TCM (47). The general process of network pharmacology research includes the following technical links: the collection of active ingredients, the collection of target groups of related diseases, the integration of disease targets and compound targets, network construction and gene enrichment analysis (48,49). Even though, network pharmacology has broken through the previous research pattern of single target and changed into the research model of "network target", there are still many problems in its practical application, such as incomplete database information and the lack of experimental verification (50). However, it is still an effective means to excavate new drug mechanisms in TCM. Therefore, this study was based on network pharmacology to construct the relevant network of YSXZ for the treatment of AKI, so as to explore the molecular biological mechanism behind it.

MAPK can be expressed in all eukaryotic cells. Its basic composition is a 3-level kinase mode, including MAPK kinase kinase (*MAPKKK*), MAPK kinase (*MAPKK*), and *MAPK*. These 3 kinases are in turn activated and progressively amplified to regulate important physiological and pathological processes such as cell proliferation, differentiation, environmental stress adaptation, and

inflammatory responses. *JNK*, *ERK* and *p38* are 3 important branches of this pathway (51). The MAPK pathway is closely related to the occurrence and development of AKI. Lin *et al.* (52) found that the expression of *MAPK* kinase was significantly upregulated in the DDP-induced AKI *in vivo* model. Sun *et al.* (53) observed that the phosphorylation ratios of *ERK1/2*, *JNK*, and *p38* were significantly upregulated in the *in vivo* and *in vitro* models of IRI-induced AKI. Thus, the *MAPK* pathway is the key pathway to prevent and treat AKI.

In recent years, it has been found that the *MAPK* pathway also plays an important role in cell senescence. Under external stimuli, *MAPKs* will act as sensors to identify the type and extent of damage and help determine what programs cells will perform to deal with damage such as cell proliferation, differentiation, apoptosis, aging, or others. If cellular senescence is performed, *MAPK* is directly involved in the generation of various traits of senescence. Firstly, *ERK* and *p38* can directly or indirectly phosphorylate *p53*, increase the expression of *p16* and *p21* mRNA, and arrest the cell cycle. Secondly, *MAPKs* function via NF-κB-dependent and independent pathways to control the production and secretion of SASP. Thirdly, *MAPK* is the core anti-apoptotic phenotype, which can ensure the long-term survival of senescent cells (54).

This experiment was the first to study the effect of YSXZ on the *in vitro* cytological model of DDP-induced renal injury. It was found that after DDP interferes with RTECs, the cell viability decreased in a concentration dependent manner, and at the same time, a series of aging related manifestations appeared in RTECs. YSXZ can reduce SA-β-Gal staining area and aging related proteins *p16*, *p21*, *p53*, *γ-H2AX* expression levels, reverse the phenomenon of S-phase arrest of cell cycle after DDP intervention, and reduce the aging-related secretion phenotype *IL-1β* and *IL-6*. Therefore, it is speculated that the mechanism of YSXZ in treating DDP-mediated renal injury may be related to cell senescence. Next, 214 core targets of the YSXZ recipe for the treatment of AKI were screened out using network pharmacology, and through GO analysis and KEGG analysis, it was found that these core targets were concentrated in the *MAPK* pathway and *Pi3K* pathway. In response to this finding, we applied western blot to verify the experiment, and found that after DDP stimulation, the *MAPK* pathway was activated. After the intervention of YSXZ, the expression of *JNK*, *p38*, and *ERK1/2* were significantly down regulated.

Conclusions

Therefore, we concluded that YSXZ ameliorated the development of the DDP-induced AKI by attenuating RTEC senescence via alleviating the activation of *MAPK* pathway.

Acknowledgments

Funding: This work was supported by the National Natural Science Foundation of China (No. 81774038 to Xiaoli Nie) and the Natural Science Foundation of Guangdong Province (Nos. 2015A020213300 and 2021A1515011672 to Xiaoli Nie).

Footnote

Reporting Checklist: The authors have completed the MDAR and ARRIVE reporting checklists. Available at https://atm.amegroups.com/article/view/10.21037/atm-22-5415/rc

Data Sharing Statement: Available at https://atm.amegroups.com/article/view/10.21037/atm-22-5415/dss

Conflicts of Interest: All authors have completed the ICMJE uniform disclosure form (available at https://atm.amegroups.com/article/view/10.21037/atm-22-5415/coif). XN reports that this work was supported by the National Natural Science Foundation of China (No. 81774038) and the Natural Science Foundation of Guangdong Province (Nos. 2015A020213300 and 2021A1515011672). The other authors have no conflicts of interest to declare.

Ethical Statement: The authors are accountable for all aspects of the work in ensuring that questions related to the accuracy or integrity of any part of the work are appropriately investigated and resolved. Animal experiments were performed under a project license (No. L2022-065) granted by Laboratory Animal Welfare and Ethics Committee of Integrated Hospital of Traditional Chinese Medicine, Southern Medical University, and was carried out in compliance with the relevant regulations of the Experimental Animal Ethics and Welfare Committee of Southern Medical University.

References

1. Zhou C, Wang Z, Sun Y, et al. Sugemalimab versus placebo, in combination with platinum-based chemotherapy, as first-line treatment of metastatic non-small-cell lung cancer (GEMSTONE-302): interim and final analyses of a double-blind, randomised, phase 3 clinical trial. Lancet Oncol 2022;23:220-33.
2. Kim R, An M, Lee H, et al. Early Tumor-Immune Microenvironmental Remodeling and Response to First-Line Fluoropyrimidine and Platinum Chemotherapy in Advanced Gastric Cancer. Cancer Discov 2022;12:984-1001.
3. Colombo N, Dubot C, Lorusso D, et al. Pembrolizumab for Persistent, Recurrent, or Metastatic Cervical Cancer. N Engl J Med 2021;385:1856-67.
4. Tang Q, Wang X, Jin H, et al. Cisplatin-induced ototoxicity: Updates on molecular mechanisms and otoprotective strategies. Eur J Pharm Biopharm 2021;163:60-71.
5. Acklin S, Xia F. The Role of Nucleotide Excision Repair in Cisplatin-Induced Peripheral Neuropathy: Mechanism, Prevention, and Treatment. Int J Mol Sci 2021;22:1975.
6. Aapro M, Navari RM, Roeland E, et al. Efficacy of intravenous NEPA, a fixed NK(1)/5-HT(3) receptor antagonist combination, for the prevention of chemotherapy-induced nausea and vomiting (CINV) during cisplatin- and anthracycline cyclophosphamide (AC)-based chemotherapy: A review of phase 3 studies. Crit Rev Oncol Hematol 2021;157:103143.
7. Ongnok B, Chattipakorn N, Chattipakorn SC. Doxorubicin and cisplatin induced cognitive impairment: The possible mechanisms and interventions. Exp Neurol 2020;324:113118.
8. Motwani SS, McMahon GM, Humphreys BD, et al. Development and Validation of a Risk Prediction Model for Acute Kidney Injury After the First Course of Cisplatin. J Clin Oncol 2018;36:682-8.
9. Gao XS, Boere IA, van Beekhuizen HJ, et al. Acute and long-term toxicity in patients undergoing induction chemotherapy followed by thermoradiotherapy for advanced cervical cancer. Int J Hyperthermia 2022;39:1440-8.
10. Landau SI, Guo X, Velazquez H, et al. Regulated necrosis and failed repair in cisplatin-induced chronic kidney disease. Kidney Int 2019;95:797-814.
11. Duan ZY, Liu JQ, Yin P, et al. Impact of aging on the risk of platinum-related renal toxicity: A systematic review and meta-analysis. Cancer Treat Rev 2018;69:243-53.
12. Di Micco R, Krizhanovsky V, Baker D, et al. Cellular senescence in ageing: from mechanisms to therapeutic opportunities. Nat Rev Mol Cell Biol 2021;22:75-95.
13. Watts G. Leonard Hayflick and the limits of ageing. Lancet 2011;377:2075.
14. Li Q, Hagberg CE, Silva Cascales H, et al. Obesity and hyperinsulinemia drive adipocytes to activate a cell cycle program and senesce. Nat Med 2021;27:1941-53.
15. Al-Dabet MM, Shahzad K, Elwakiel A, et al. Reversal of the renal hyperglycemic memory in diabetic kidney disease by targeting sustained tubular p21 expression. Nat Commun 2022;13:5062.
16. Yang L, Besschetnova TY, Brooks CR, et al. Epithelial cell cycle arrest in G2/M mediates kidney fibrosis after injury. Nat Med 2010;16:535-43, 1p following 143.
17. Muggia FM, Bonetti A, Hoeschele JD, et al. Platinum Antitumor Complexes: 50 Years Since Barnett Rosenberg's Discovery. J Clin Oncol 2015;33:4219-26.
18. Manohar S, Leung N. Cisplatin nephrotoxicity: a review of the literature. J Nephrol 2018;31:15-25.
19. Tang C, Livingston MJ, Safirstein R, et al. Cisplatin nephrotoxicity: new insights and therapeutic implications. Nat Rev Nephrol 2023;19:53-72.
20. Fang CY, Lou DY, Zhou LQ, et al. Natural products: potential treatments for cisplatin-induced nephrotoxicity. Acta Pharmacol Sin 2021;42:1951-69.
21. Qu X, Gao H, Tao L, et al. Astragaloside IV protects against cisplatin-induced liver and kidney injury via autophagy-mediated inhibition of NLRP3 in rats. J Toxicol Sci 2019;44:167-75.
22. Su J, He T, You J, et al. Therapeutic effect and underlying mechanism of Shenkang injection against cisplatin-induced acute kidney injury in mice. J Ethnopharmacol 2023;301:115805.
23. Ru J, Li P, Wang J, et al. TCMSP: a database of systems pharmacology for drug discovery from herbal medicines. J Cheminform 2014;6:13.
24. Lipinski CA, Lombardo F, Dominy BW, et al. Experimental and computational approaches to estimate solubility and permeability in drug discovery and

development settings. Adv Drug Deliv Rev 2001;46:3-26.
25. Stelzer G, Rosen N, Plaschkes I, et al. The GeneCards Suite: From Gene Data Mining to Disease Genome Sequence Analyses. Curr Protoc Bioinformatics 2016;54:1.30.1-1.30.33.
26. Amberger JS, Hamosh A. Searching Online Mendelian Inheritance in Man (OMIM): A Knowledgebase of Human Genes and Genetic Phenotypes. Curr Protoc Bioinformatics 2017;58:1.2.1-1.2.12.
27. Zhou Y, Zhang Y, Lian X, et al. Therapeutic target database update 2022: facilitating drug discovery with enriched comparative data of targeted agents. Nucleic Acids Res 2022;50:D1398-407.
28. Piñero J, Saüch J, Sanz F, et al. The DisGeNET cytoscape app: Exploring and visualizing disease genomics data. Comput Struct Biotechnol J 2021;19:2960-7.
29. Szklarczyk D, Morris JH, Cook H, et al. The STRING database in 2017: quality-controlled protein-protein association networks, made broadly accessible. Nucleic Acids Res 2017;45:D362-8.
30. Wang Y, Qian X. Functional module identification in protein interaction networks by interaction patterns. Bioinformatics 2014;30:81-93.
31. Hu J, Wu TM, Li HZ, et al. The synthesis, structure-toxicity relationship of cisplatin derivatives for the mechanism research of cisplatin-induced nephrotoxicity. Bioorg Med Chem Lett 2017;27:3591-4.
32. Duffy EA, Fitzgerald W, Boyle K, et al. Nephrotoxicity: Evidence in Patients Receiving Cisplatin Therapy. Clin J Oncol Nurs 2018;22:175-83.
33. Moujaber O, Fishbein F, Omran N, et al. Cellular senescence is associated with reorganization of the microtubule cytoskeleton. Cell Mol Life Sci 2019;76:1169-83.
34. Narita M, Nũnez S, Heard E, et al. Rb-mediated heterochromatin formation and silencing of E2F target genes during cellular senescence. Cell 2003;113:703-16.
35. Dimri GP, Lee X, Basile G, et al. A biomarker that identifies senescent human cells in culture and in aging skin in vivo. Proc Natl Acad Sci U S A 1995;92:9363-7.
36. Chambers CR, Ritchie S, Pereira BA, et al. Overcoming the senescence-associated secretory phenotype (SASP): a complex mechanism of resistance in the treatment of cancer. Mol Oncol 2021;15:3242-55.
37. Childs BG, Gluscevic M, Baker DJ, et al. Senescent cells: an emerging target for diseases of ageing. Nat Rev Drug Discov 2017;16:718-35.
38. Li C, Xie N, Li Y, et al. N-acetylcysteine ameliorates cisplatin-induced renal senescence and renal interstitial fibrosis through sirtuin1 activation and p53 deacetylation. Free Radic Biol Med 2019;130:512-27.
39. Liu H, Lü Z, Tian C, et al. Mechanism of Shenbing decoction III in the treatment of proteinuria in chronic kidney disease: a network pharmacology-based study. Nan Fang Yi Ke Da Xue Xue Bao 2019;39:227-34.
40. Song Y, Hu T, Gao H, et al. Altered metabolic profiles and biomarkers associated with astragaloside IV-mediated protection against cisplatin-induced acute kidney injury in rats: An HPLC-TOF/MS-based untargeted metabolomics study. Biochem Pharmacol 2021;183:114299.
41. Zhang Y, Qin S, Song Y, et al. Alginate Oligosaccharide Alleviated Cisplatin-Induced Kidney Oxidative Stress via Lactobacillus Genus-FAHFAs-Nrf2 Axis in Mice. Front Immunol 2022;13:857242.
42. Hopkins AL. Network pharmacology: the next paradigm in drug discovery. Nat Chem Biol 2008;4:682-90.
43. Klipp E, Wade RC, Kummer U. Biochemical network-based drug-target prediction. Curr Opin Biotechnol 2010;21:511-6.
44. Sun X, Zhang Y, Zhou Y, et al. NPCDR: natural product-based drug combination and its disease-specific molecular regulation. Nucleic Acids Res 2022;50:D1324-33.
45. Wang Y, Yang H, Chen L, et al. Network-based modeling of herb combinations in traditional Chinese medicine. Brief Bioinform 2021;22:bbab106.
46. Tang YP, Xu DQ, Yue SJ, et al. Modern research thoughts and methods on bio-active components of TCM formulae. Chin J Nat Med 2022;20:481-93.
47. Li S, Zhang B. Traditional Chinese medicine network pharmacology: theory, methodology and application. Chin J Nat Med 2013;11:110-20.
48. Noor F, Tahir Ul Qamar M, Ashfaq UA, et al. Network Pharmacology Approach for Medicinal Plants: Review and Assessment. Pharmaceuticals (Basel) 2022;15:572.
49. Yuan Z, Pan Y, Leng T, et al. Progress and Prospects of Research Ideas and Methods in the Network Pharmacology of Traditional Chinese Medicine. J Pharm Pharm Sci 2022;25:218-26.
50. Wang X, Wang ZY, Zheng JH, et al. TCM network pharmacology: A new trend towards combining computational, experimental and clinical approaches. Chin J Nat Med 2021;19:1-11.
51. Hepworth EMW, Hinton SD. Pseudophosphatases as Regulators of MAPK Signaling. Int J Mol Sci 2021;22:12595.
52. Lin WH, Jiang WP, Chen CC, et al. Renoprotective

Effect of Pediococcus acidilactici GKA4 on Cisplatin-Induced Acute Kidney Injury by Mitigating Inflammation and Oxidative Stress and Regulating the MAPK, AMPK/SIRT1/NF-κB, and PI3K/AKT Pathways. Nutrients 2022;14:2877.
53. Sun W, Choi HS, Kim CS, et al. Maslinic Acid Attenuates Ischemia/Reperfusion-Induced Acute Kidney Injury by Suppressing Inflammation and Apoptosis Through Inhibiting NF-κB and MAPK Signaling Pathway. Front Pharmacol 2022;13:807452.
54. Anerillas C, Abdelmohsen K, Gorospe M. Regulation of senescence traits by MAPKs. Geroscience 2020;42:397-408.

(English Language Editor: J. Jones)

Cite this article as: Zhang Q, Qi J, Luo Q, Wu M, Zhang L, Qin L, Nie X. Yishen Xiezhuo formula ameliorates the development of cisplatin-induced acute kidney injury by attenuating renal tubular epithelial cell senescence. Ann Transl Med 2022;10(24):1392. doi: 10.21037/atm-22-5415

